



**HAL**  
open science

# Slow Transients and Metastability in Wormlike Micelle Rheology

C. Grand, J. Arrault, M. Cates

► **To cite this version:**

C. Grand, J. Arrault, M. Cates. Slow Transients and Metastability in Wormlike Micelle Rheology. Journal de Physique II, 1997, 7 (8), pp.1071-1086. 10.1051/jp2:1997172 . jpa-00248498

**HAL Id: jpa-00248498**

**<https://hal.science/jpa-00248498>**

Submitted on 4 Feb 2008

**HAL** is a multi-disciplinary open access archive for the deposit and dissemination of scientific research documents, whether they are published or not. The documents may come from teaching and research institutions in France or abroad, or from public or private research centers.

L'archive ouverte pluridisciplinaire **HAL**, est destinée au dépôt et à la diffusion de documents scientifiques de niveau recherche, publiés ou non, émanant des établissements d'enseignement et de recherche français ou étrangers, des laboratoires publics ou privés.

# Slow Transients and Metastability in Wormlike Micelle Rheology

C. Grand <sup>(1,2)</sup>, J. Arrault <sup>(1,\*)</sup> and M.E. Cates <sup>(1)</sup>

<sup>(1)</sup> Department of Physics and Astronomy, University of Edinburgh, JCMB King's Buildings, Mayfield Road, Edinburgh EH9 3JZ, UK

<sup>(2)</sup> Centre de Recherche Paul Pascal (CNRS), avenue Schweitzer, 33600 Pessac, France

(Received 28 February 1997, accepted 5 May 1997)

PACS.82.70.-y - Disperse systems

PACS.83.10.Nn - Polymer dynamics

PACS.83.50.By - Transient deformation and flow; time dependent properties:  
start-up, stress relaxation, creep, recovery, etc.

**Abstract.** — The steady-state nonlinear rheology of wormlike micellar systems is thought to be subject to shear banding (the underlying shear stress *vs.* strain rate curve  $\sigma(\dot{\gamma})$  is nonmonotonic). Shear banding may result in a plateau ( $\sigma(\dot{\gamma}) = \sigma_p$ ) in the *measured* flow curve (at controlled *mean* strain rate  $\dot{\gamma}$ ). We present new rheological data for aqueous CPyCl/NaSal (100 mM/60 mM). Steady-state flow curves published previously for this system (Rehage H. and Hoffmann H., *Mol. Phys.* **74** (1991) 933) have since been interpreted as shear-banded flow with “top-jumping”, in which the steady-state shear rate  $\dot{\gamma}_1$  in the low shear band is the largest possible ( $\dot{\gamma}_1 = \dot{\gamma}_1^{\max}$ ,  $\sigma_p = \sigma_{\max}$ ). That would rule out the existence of a metastable branch with a stress larger than  $\sigma_p$ . We show that such a branch does, however, exist (for temperatures in the range 20 – 25 °C). Similar results are found for a 100 mM/75 mM system. The time scale for relaxation of a metastable state onto true steady state flow,  $\tau_{ss}$ , is far longer than the Maxwell time of the fluid; this is consistent with shear banding. We observe  $\tau_{ss} \sim (\dot{\gamma} - \dot{\gamma}_c)^{-p}$  in the metastable regime ( $\dot{\gamma} \geq \dot{\gamma}_1$ ), with  $p$  an exponent that depends on composition and temperature. The “critical” shear rate  $\dot{\gamma}_c$  is in some cases less than  $\dot{\gamma}_1$  so that no actual divergence of  $\tau_{ss}$  occurs. In at least one case, though, there is evidence for a physical divergence ( $\dot{\gamma}_c > \dot{\gamma}_1$ ) accompanied by a small window of shear rates,  $\dot{\gamma}_1 \leq \dot{\gamma} \leq \dot{\gamma}_c$ , for which  $\tau_{ss}$  is effectively infinite. In some respects the observed behaviour resembles that reported previously (Berret J.-F., Roux D.C. and Porte G., *J. Phys. II France* **4** (1994) 1261) for equimolar CPyCl/NaSal in 0.5 M NaCl. Those results were interpreted in terms of nucleation and growth of a shear-induced nematic phase. However the same explanation is unlikely for the low weight fractions ( $\phi \leq 5\%$ ) used in our study.

## 1. Introduction

The rheology of wormlike micelles has attracted the attention of many workers in recent years. Under suitable conditions, these systems exhibit viscoelastic phases in which the micelles are highly entangled [1]. In the linear response region, such materials often show behaviour remarkably close to that of an ideal Maxwell fluid (mono-exponential stress decay, with a relaxation time  $\tau_M$ ). This behaviour has been explained by a model which combines the reptation

---

(\*) Author for correspondence (e-mail: j.arrault@ph.ed.ac.uk)

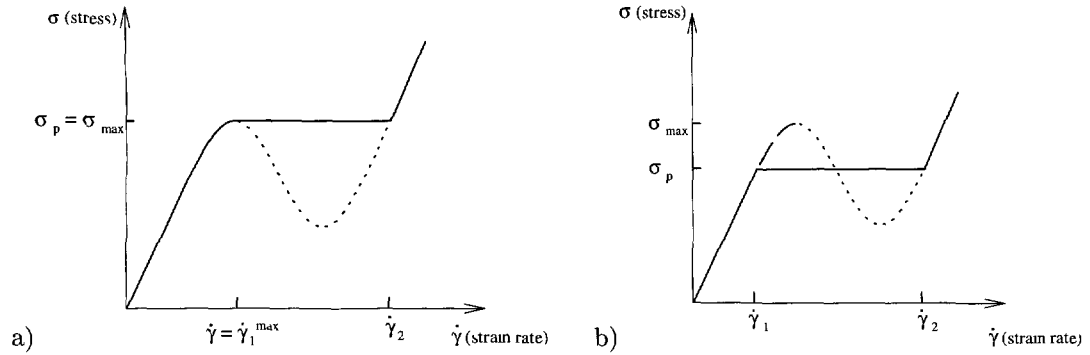


Fig. 1. — a) A nonmonotonic stress *vs.* strain rate curve; the dotted part is unstable. In a banded flow, regions of strain rate  $\dot{\gamma}_1, \dot{\gamma}_2$  coexist to give a macroscopic mean strain rate  $\dot{\gamma}$  which is fixed (under controlled strain rate conditions). The observed flow curve (solid) corresponds to “top jumping”:  $\sigma_p = \sigma_{\max}$ . b) The same, but with some other selection mechanism giving a plateau stress  $\sigma_p$  less than the maximum. This allows a metastable branch (dashed) to develop. Depending on lifetimes of metastable states, the observable branch could, but need not, extend as far as  $\sigma_{\max}$  as shown (*cf.* Fig. 12 below).

mechanism for relaxation of entanglements with the reversible scission of the linear micellar aggregates [2]. The same model, applied to the nonlinear flow regime, predicts some much more complicated effects [3, 4]. Specifically it is found that the stress *vs.* strain-rate curve,  $\sigma(\dot{\gamma})$  in homogeneous steady shear flow is nonmonotonic. The decreasing part of such a curve is unstable [5]; to maintain a steady flow, a system subjected to a mean strain rate lying in this region may split into “shear bands” of low and high strain rate  $\dot{\gamma}_1$  and  $\dot{\gamma}_2$ : see Figure 1. (This assumes that (as shown) the underlying flow curve eventually increases again at high  $\dot{\gamma}$ , though mechanistic details of this remain obscure [6].) The occurrence of shear-bands (or at least, a strongly inhomogeneous shear rate in steady state), for micellar systems undergoing cylindrical Couette flow, is now established by experiment. The evidence comes from birefringence microscopy [7] and especially NMR velocimetry [8, 9], although the latter also reveals a number of unexplained features [8, 10]. Very recent NMR data [11] shows that the same occurs in a cone/plate geometry in which the *stress* field is very close to being ideally homogeneous.

If shear-banding happens, there remains the issue of selection: what are the two shear-rates, or (equivalently) what is the value of the stress  $\sigma_p$  shared by the two bands? The simplest ansatz (known as top-jumping) postulates that  $\sigma_p$  is at the maximum of the underlying (nonmonotonic) flow curve (Fig. 1a). On this basis, good quantitative agreement was found [4] between the predictions of the reptation-reaction model and the data of Rehage and Hoffmann [12] on the system CPyCl/NaSal (100 mM/60 M) in water. Qualitatively similar results have been reported for several other systems [13].

However, recent work based on solving numerically the constitutive equation for micelles [14], and also theories which allow for nonlocal constitutive behaviour [14–16], suggest that the top-jumping criterion does not, in general, identify the true steady-state banded flow under conditions of homogeneous stress. The question of band selection therefore remains open. Since it is not possible in a real rheometer to achieve a completely uniform stress field, small perturbations to planar Couette flow could be important [17]. Also, in principle the criterion could depend on  $\dot{\gamma}$  in such a way that a ramp [16, 17], rather than a plateau, would be seen in the measured flow curve; but if this occurs in micelles, the ramp seems to be relatively flat.

(Although we below detect departures from a completely horizontal plateau in some of our data, for simplicity in our discussions we mainly ignore this slight slope.)

Experimentally, a careful series of experiments by Berret *et al.* [18] have revealed flow curves in which clear departures from top jumping are seen. In these curves, the shear stress  $\sigma_p$  in the plateau region, corresponding to banded flow, lies well below the stress maximum on the underlying flow curve. (In the reptation-reaction model, this maximum occurs at  $\dot{\gamma} = \dot{\gamma}_1^{\max} = 2.6/\tau_M$  with  $\sigma = \sigma_{\max} = 0.67G_0$ ; here  $G_0$  is the high frequency plateau modulus defined as usual by *linear* viscoelastic measurements [4].) This behaviour is accompanied by a sharp corner on the measured flow curve at  $\dot{\gamma}_1$  (Fig. 1b). These experiments, however, are on relatively concentrated systems (weight fraction  $\phi \sim 5\text{--}30\%$ ), and although their chemistry is similar, it is not identical to the CPyCl/NaSal systems studied by Rehage and Hoffmann, and below (excess salt is present). The results of Berret *et al.* were originally interpreted as evidence against a purely rheological instability and in favour of a somewhat different mechanism, involving the shear-induced nucleation and growth of a nematic phase [18]. The issue here is not whether the micelles in the high-shear band ( $\dot{\gamma} = \dot{\gamma}_2$ ) formally have nematic order (in view of the flow this is inevitable) but whether the banding instability is best regarded as a flow-induced perturbation to a static phase transition, or as “purely” flow-induced. In practice the distinction between these viewpoints is certainly not sharp [19].

## 2. The Present Study

In the present work, we examine experimentally a 100 mM/60 mM CPyCl/NaSal system at various temperatures, and also present results for a slightly different composition (100 mM/75 mM). We show that the true steady-state flow curve does not correspond to top-jumping ( $\sigma_p = \sigma_{\max}$ ) but to a distinctly lower value of  $\sigma_p$ . When  $\sigma_p$  is close to, but below,  $\sigma_{\max}$ , the two behaviours may be hard to distinguish from the flow curve alone. After all, the predicted value  $\sigma_{\max} = 0.67G_0$  is somewhat model dependent [3]. Likewise, although in principle there is for  $\sigma_p < \sigma_{\max}$  a finite change in slope at the plateau onset, this may be too small to measure. A much better test for whether in reality  $\sigma_p < \sigma_{\max}$  is to look for a metastable branch of the flow curve with  $\sigma > \sigma_p$  (See Fig. 1b). We find that for temperatures between 20 and 25 °C. such a branch is readily observed. This precludes top jumping as the criterion for band selection in our systems. We also find that, to see the true steady-state behaviour, one has to perform measurements *exceedingly slowly*. The time-scale  $\tau_{ss}$  for equilibration onto the steady state, reported below, can be hundreds or thousands of times longer than the Maxwell time  $\tau_M$  (which is typically a few seconds), and in the 100/60 system appears unmeasurably long for a small window of mean strain rates  $\dot{\gamma}$  just above  $\dot{\gamma}_1$ . Consistent with these findings, we also observe that (a) in fast stress-controlled scans (roughly one data point per Maxwell time), a flow curve resembling top-jumping can be recorded; (b) under strain-rate control, even in relatively slow scans at increasing strain rate, it is normal to obtain a bump in the flow curve, as has occasionally been reported before [9]. This bump is rather reproducible, but disappears if the scan is done subsequently under *decreasing* strain rate.

In the light of our results, one may question to what extent the original data of Rehage and Hoffmann for 100/60 mM CPyCl/NaSal [12] represents a true steady state flow curve. At that time the theoretical suggestion of shear-banding in wormlike micelles had not yet been made, so it would have been normal to assume that, for each shear rate, the steady state flow was reached within a few Maxwell times. Indeed, in their paper, Rehage and Hoffmann included startup curves for which data is not plotted beyond ten Maxwell times (Ref. [12], Fig. 32). Our own results suggest that the final steady state is achieved only at much longer times than this (and also those used for the flow curves reported in [9]). It should also be noted, however, that

the system we study, and that studied by Rehage and Hoffmann may not be exactly the same. It is widely known that systems containing the salicylate ion ( $\text{Sal}^-$ ) are prone to various kinds of aging and degradation, and may also be very sensitive to impurity levels [20].

In what follows, we summarize our experimental setup (Sect. 3) and then present  $\sigma(\dot{\gamma})$  curves measured under carefully specified conditions (Sect. 4). In Section 5 we present results for the transient approach to the steady state, highlighting the extremely long relaxation times  $\tau_{\text{ss}}$ . In Section 6 we discuss the shape of the transient response, and compare with a functional form suggested by the work of Berret *et al.* [18]. The dependence of the relaxation time  $\tau_{\text{ss}}$  on  $\dot{\gamma}$  is also discussed in detail. Section 7 contains our concluding remarks.

### 3. Experimental

The aqueous surfactant solutions chosen were (a) 100 mM cetylpyridinium chloride/60 mM sodium salicylate, and (b) the same but with 100/75 mM. The chemicals were supplied by Aldrich and by BDH and used without further purification. Samples were made up with once-distilled water. The weight fractions of the two samples are respectively 4.6% and 4.8%. The 100/60 system undergoes a phase transition (Krafft point) at 19 °C (this temperature is slightly lower, 18 °C, for 100/75). This transition is strongly first order and does not appear to be involved in any of the phenomena occurring under flow at higher temperature. Measurements were made for several temperatures in the range 19–25 °C; this was controlled by a Peltier cell and/or a thermal jacket ( $\pm 0.1$  °C accuracy).

Most of our rheological data was obtained on a TA Carrimed CSL<sup>2</sup>100 Rheometer, with either a cone and plate cell (6 cm diameter, angle 2°) or a Couette cell with a gap of 1 mm and inner radius 24 mm. The inner cylinder is terminated at the base by a cone and plate region (Mooney cell). This machine is intrinsically a stress-controlled design but software for strain-rate control was used. An inbuilt over-ride prevents the latter from being used at too low a shear rate ( $\dot{\gamma} \leq 0.29 \text{ s}^{-1}$ ): apart from this restriction we encountered no problems imposing strain-rate control in this machine. (The main drawback of software control is insensitivity to *fast* transients, which are not our focus in this work.) To be sure on this point we performed a small number of measurements on a Rheometrics Fluid Spectrometer (at CRPP, Bordeaux), using a Couette cell of diameter 34 mm with a gap of 2 mm. The inner cylinder has a “dimple” on its lower face to eliminate contributions from the fluid beneath. This machine is intrinsically strain-rate controlled; apart from some extra short-time-scale features, this produced similar relaxation curves and relaxation times to the Carrimed data.

To characterize our samples, we measured first their linear viscoelastic spectra. Representative curves are shown in Cole-Cole form in Figure 2. These show good, but not perfect, Maxwell behaviour. The value of  $G_0$  can be found by fitting to a semicircle and finding the intersection point on the horizontal axis [1, 21]. Our  $G_0 = 27 \text{ Pa}$  value for the 100/60 system is somewhat below that of Rehage and Hoffmann ( $G_0 = 31 \text{ Pa}$ ) [12]. A rather larger value was reported by Callaghan *et al.* [9]. For the 100/75 system we measured  $G_0 = 36 \text{ Pa}$ . We found no appreciable dependence of  $G_0$  on  $T$  in the temperature range studied. Note the substantial difference in  $G_0$  on switching from 0.6 to 0.75 Sal/CPyCl ratio. Since (in this strongly entangled regime)  $G_0$  depends only on the entanglement mesh size and not on the micelle length [1], this can be explained only by assuming that the persistence length is rather different in the two samples. This is consistent with complexation of the counterions at the micelle surface which may change its stiffness. Also obtained from the linear viscoelastic spectra are values of the Maxwell time, as shown in Table I. Those for 100/60 are once again similar but not identical to values reported previously.

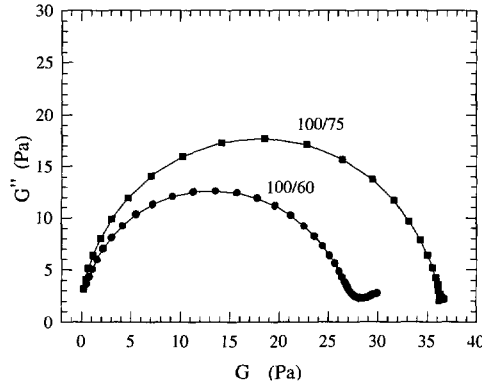


Fig. 2. — Cole-Cole plots of linear viscoelastic spectra for 100/60 and 100/75 at 20 °C. (In this representation, the Maxwell model describes a semicircle. The solid lines are to guide the eye.)

Table I. — *Maxwell times for stated compositions/temperatures.*

$T$	19 °C	20 °C	23.5 °C	25 °C
100/60 mM	-	4.5 s	2.5 s	1.7 s
100/75 mM	1.7 s	1.2 s	0.6 s	0.4 s

In what follows, we use the measured plateau modulus values to scale all the measured stresses; this is done separately for each filling of the rheometer cell. The procedure eliminates possible systematic errors from variation in the filling level of the cell (which is hard to control precisely for these highly viscous fluids), and eases comparison between the various curves.

#### 4. Nonlinear Viscoelasticity

Typical  $\sigma(\dot{\gamma})$  flow curves are shown in Figures 3-5. Because of the slow transients, it is important to specify carefully the conditions under which these curves are measured.

4.1. SYSTEM 100/60 AT 23.5 °C. — Refer first to Figure 3a, which shows three different types of run for 100/60 at 23.5 °C in a cone and plate geometry. The uppermost curve is measured under controlled stress conditions, if the stress is increased relatively fast (ten seconds between one data point and the next). This curve shows a smooth transition to a plateau, not unlike that expected if the shear-bands are selected according to the top-jumping criterion. However, this is definitely a nonequilibrium curve; the “apparent plateau” stress  $\sigma_p^{\text{app}}$  is about  $0.7-0.8G_0$  and is sensitive to the rate of sweep and also the cell geometry. (Apart from this value, nearly identical curves were also measured for the Couette-Mooney cell.)

By choosing instead a strain-rate sweep and varying the flow conditions much more slowly (about 100 s per data point), a quite different curve is measured. On increasing strain rates, there is a bump in the stress, which beyond a certain point drops fairly sharply onto a plateau at  $\sigma_p \simeq 0.54G_0$ . The strain rate can then be increased further with barely any increase in measured stress. If the strain rate is now swept *down* from a high value, the plateau is retraced, the decreasing branch lying marginally below the increasing one. More significantly, the bump is not seen. All these effects are reproducible at the stated sweep rate.

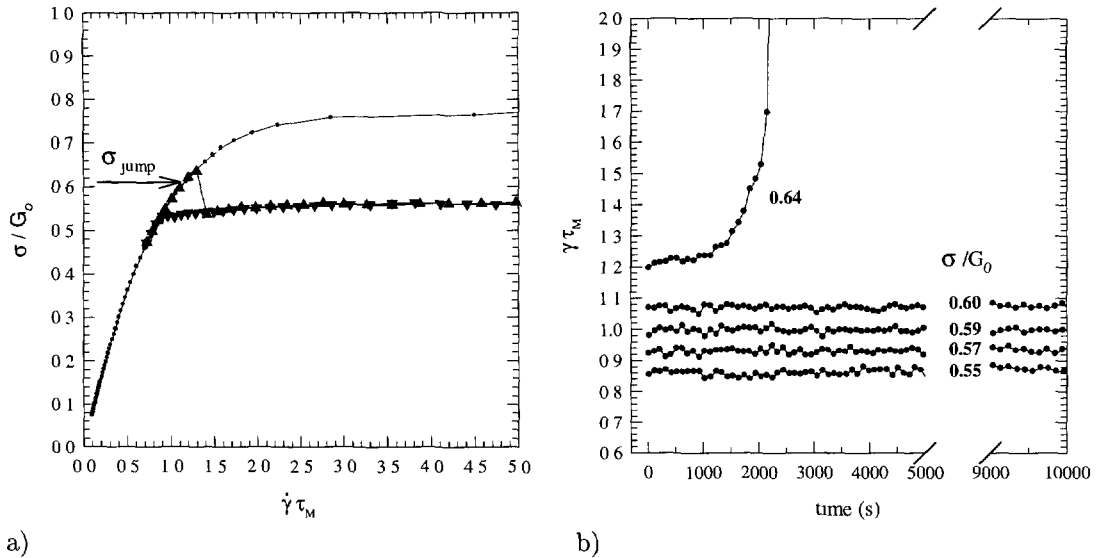


Fig. 3. — System 100/60 at 23.5 °C. a) Three “steady-state” flow curves measured under different nonequilibrium conditions as explained in the text. Circles: stress control, 10 s per data point. Triangles: controlled strain rate, 100 s per data point, increasing (upright) and decreasing (inverted). b) Startup of steady stress curve, showing the metastability of flows with  $\sigma_p < \sigma < \sigma_{\text{jump}} \simeq 0.61G_0$ . (Data from cone-plate cell and TA rheometer.)

It is interesting to perform for comparison a relatively slow stress-controlled (stress sweep) curve. The curve (not shown in Fig. 3a) follows the fast controlled stress-sweep curve up to a stress which lies clearly above  $\sigma_p$ ; the system then becomes unstable and the strain rate starts increasing very rapidly. We call the stress at which this sudden change occurs  $\sigma_{\text{jump}}$ . The measured value depends on the sweep rate, but not strongly. A more reproducible definition of  $\sigma_{\text{jump}}$  is found by observing controlled stress startup curves, as shown in Figure 3b. For stresses in the range  $\sigma_p < \sigma < \sigma_{\text{jump}}$ , the system remains for very many Maxwell times at a constant shear rate, lying on what is clearly a metastable branch of the  $\sigma(\dot{\gamma})$  curve. For  $\sigma > \sigma_{\text{jump}}$ , this does not occur; after a moderate time (which may still be long compared to the Maxwell time), the mean strain rate starts increasing rapidly until the sample is ejected from the rheometer cell. Our best estimate is  $\sigma_{\text{jump}} = 0.61G_0$  for this system.

These data establish beyond doubt that the 100/60 system does not show simple “top-jumping” at 23.5 °C. Instead the shear bands are selected in some other way. As mentioned in the introduction, this direct observation of the metastable branch is much more conclusive than a comparison of the plateau stress  $\sigma_p = 0.54G_0$  with the *theoretical* top-jumping value  $\sigma_p = \sigma_{\text{max}} = 0.67G_0$ , bearing in mind that the fluid is not perfectly Maxwellian and hence that neither the definition of  $G_0$ , nor the theoretical prefactor 0.67, can be considered precise (the latter is anyway rather model dependent [3]).

4.2. SYSTEM 100/60 AT OTHER TEMPERATURES. — Broadly similar results were found at temperatures of 20, 21 and 25 °C, although the values of  $\sigma_p$ ,  $\sigma_{\text{jump}}$  depend on temperature. Figure 4 shows cone-plate data at 20 °C, with a strain-rate controlled scan speed of 300 s per data point. (A rapid, stress-controlled scan is also shown.) Because of the software used, our strain-rate scans are limited to only a part of the range, but the data we have is consistent

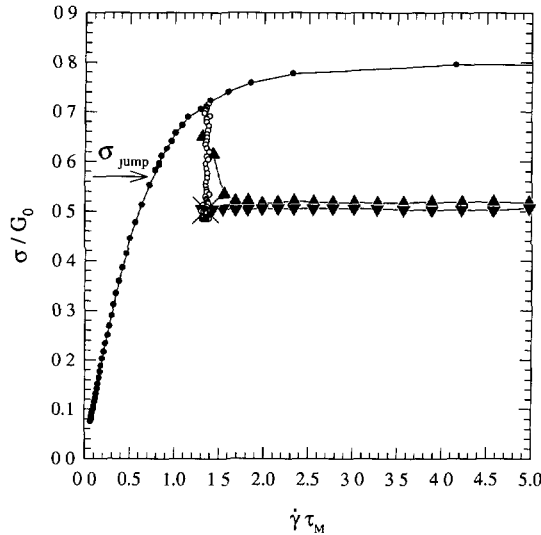


Fig. 4. — 100/60 at 20 °C: same key as in Figure 3. Open circles: trace of a strain-rate startup experiment. The long time asymptote is marked  $\times$ .

with the same scenario as seen for  $T = 23.5$  °C. In this case we find  $\sigma_p = 0.50G_0$  and  $\sigma_{\text{jump}} = 0.57G_0$ . Also shown on this plot is the trace of a strain-rate startup experiment. In other words, a steady strain rate is initiated and the observed (time-dependent) stress points are plotted, forming a vertical line segment. The upper end of this lies near the “apparent” steady state flow curve measured with a fast scan. The trace terminates at long times on the plateau (marked  $\times$ ). We will use similar plots in the next section when discussing transient behaviour; meanwhile, note that our strain-control software is working well (the line of measured strain-rates is vertical as it should be).

4.3. SYSTEM 100/75. — The behaviour of this system shows a broadly similar scenario to that found for 100/60. Figure 5 shows upward and downward strain-sweep curves (about 200 s per data point) at 19 °C, and also the trace of a startup curve. In this case the difference between  $\sigma_{\text{jump}}$  (defined as the point at which instability sets in during a slow stress sweep) and  $\sigma_p$  is less clear. The situation is delicate because the stress “plateau” is for this system not completely flat. To the observed accuracy  $\sigma_{\text{jump}}$  is very close to the steady-state shear stress observed for high strain rates, which is very slightly above that found for low ones. However, since we do not understand why these two quantities are different, we make no distinction between  $\sigma_{\text{jump}}$  and  $\sigma_p$  for this system. For the 100/75 composition, just as for 100/60 there is a noticeable temperature dependence of  $\sigma_p$ .

## 5. Transient *vs.* True Steady-State Behaviour

In the datasets discussed above, we have specified the rate at which the curves were taken. The curves that most resemble top-jumping (with  $\sigma_p = \sigma_p^{\text{app}}$ ) are clearly not steady state. The remainder were taken more slowly, at a rate which *would normally be expected* to yield true steady-state curves, if there were not processes present with relaxation time-scales far longer than the Maxwell times of the fluid (listed in Tab. I). In fact, slow processes are certainly

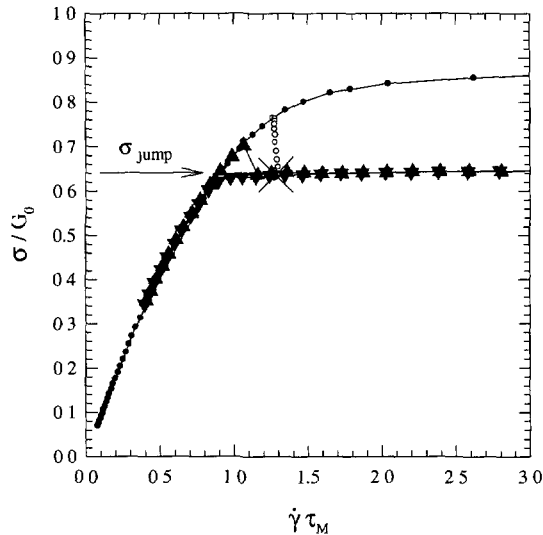


Fig. 5. — System 100/75 at 19 °C. Filled circles: stress controlled (fast scan). Triangles (inverted triangles): rising (decreasing) strain sweep curve, 200 s per data point. Open circles: startup of steady shear curve showing decay of the stress onto the plateau, marked  $\times$  (see text).

present, and they are particularly slow near the metastable branch of the flow curve. This is why this part of the curve can be measured rather easily, either in a fast controlled stress scan, or even in a slow one (for 100/60 at least, up to  $\sigma = \sigma_{\text{jump}}$ ). The metastable branch also shows up in an increasing strain rate sweep at controlled strain rate, giving rise to the bump in the measured curve. Presumably the slow relaxation times are associated with establishment of a banded flow. If so, it is not surprising that the bump is not retraced on a downward sweep (at controlled strain-rate) since a banded flow is then already present in the system. Because the transient results for it are slightly simpler, we discuss the 100/75 system first.

5.1. SYSTEM 100/75. — In Figure 6 we show (for the 100/75 system at 19 °C) a number of startup traces for different steady-shear conditions. Each startup curve is collapsed to a vertical line *which terminates on the plateau*. The behaviour is very striking, and confirms that in this system *all* controlled strain-rate data showing apparent steady-state stresses above  $\sigma_p$  are in fact transient data. The true steady-state flow curve consists of the classical form (Fig. 1b) with a plateau stress  $\sigma_p$  which lies clearly below the top-jumping value. (We know this, because the metastable part of the stress curve, lying above  $\sigma_p$  in the figure, is readily measured, and indeed matches the stresses measured at *early times* in the startup experiments.) The time-scales  $\tau_{\text{ss}}$  required for the final steady state to be achieved after startup are in the range 100–700 seconds (details are presented in the next section). It is therefore not surprising that the system stays on the metastable branch long enough for this to be the recorded stress at strain-rate sweep rates of 200 s per data point (Fig. 6). Broadly similar results to these were also obtained at  $T = 23.5$  °C. In all cases we found that the true steady-state flow curve does not depend appreciable on the geometry of the rheometer cell, although some of the transient data does.

5.2. SYSTEM 100/60. — Figure 7 shows similar data for the 100/60 system at  $T = 23.5$  °C. Here the situation is more complicated. For strain-rates well above  $\dot{\gamma}_1$  (well into the plateau

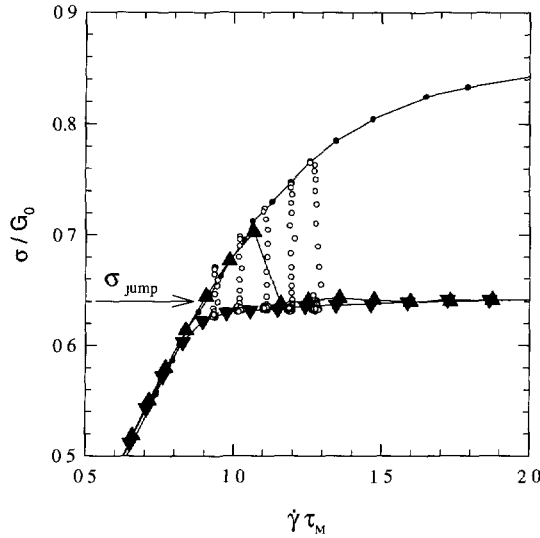


Fig. 6. — Enlarged version of Figure 5 with additional startup data (same key).

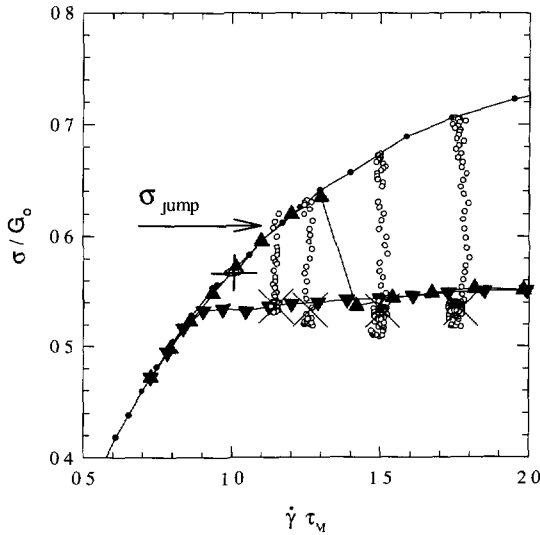


Fig. 7. — System 100/60 at 23.5 °C. Same key as Figure 5. The startup curves show either decay onto the plateau  $\times$  (higher stresses, endpoints marked  $\times$ ) or no decay (intermediate stress, endpoint marked  $+$ ). These “endpoints” are at times of order  $10^3 - 10^4 \tau_M$ .

region,  $\dot{\gamma}\tau_M > 1.1$ ), the behaviour is as before, with the startup curves terminating on the plateau stress,  $\sigma_p \approx 0.54G_0$ . (There is now an undershoot; the long time limits of the startup curves are marked  $\times$  and are indeed on or near the plateau.) However, for strain rates *very close* to but somewhat above  $\dot{\gamma}_1$  (roughly  $\dot{\gamma}_1 = 0.85/\tau_M < \dot{\gamma} < 1.1/\tau_M$ ) the startup curves appear never to decay onto the plateau. Obviously, the word “never” is dangerous. However, we have observed these systems for many hours during which the stress remains very stable

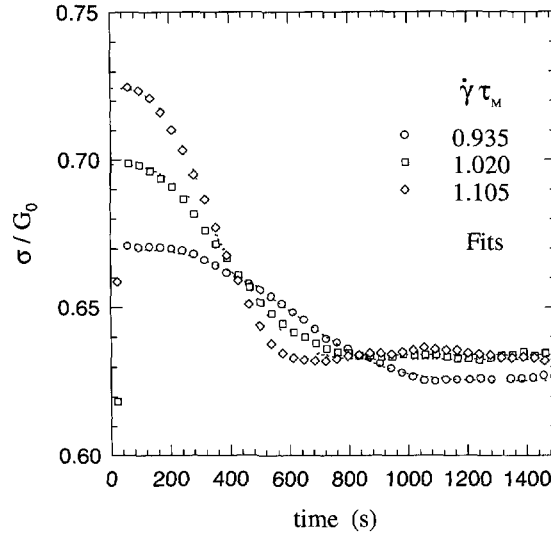


Fig. 8. — Transient response curves (startup of steady strain) for system 100/75 at 19 °C. The fitted curves are of the form of equation (1) with  $n = 3$ .

at a value discernably above  $\sigma_p$ . (The final data point on such a curve, measured after many hours, is marked +. For the full curve, see Fig. 10 below). These observations are consistent with the idea that, for a small window of strain rates above  $\dot{\gamma}_1$ , there is an effectively infinite relaxation time  $\tau_{ss}$ , in contrast to the 100/75 system.

## 6. Analysis of Transient Response

6.1. SYSTEM 100/75. — Representative startup curves are shown for this system at  $T = 19$  °C in Figure 8. These are fairly typical of those found at various temperatures. The curves are of a surprising form, similar to that seen by Berret *et al.* [18] in their study of equimolar CPyCl/NaSal in 0.5 M NaCl. After a short initial transient (of order one Maxwell time, and not detectable with our strain-control software), there is a “latency period” followed by a decay. In a few cases the transient part of the response is well fit by a Gaussian, that is

$$\sigma(t) = [\sigma(0^+) - \sigma(\infty)] \exp\left[-\left(\frac{t}{\tau_{ss}}\right)^n\right] + \sigma(\infty) \quad (1)$$

with  $n = 2$ . (This Gaussian form was theoretically motivated in Ref. [18].) However, in most cases a larger value of  $n$  gives a better fit. We chose  $n$  by eye as  $n = 2, 2.5, 3$ . Broadly similar results were found at higher temperatures.

These fits give reasonably robust estimates of the relaxation time  $\tau_{ss}$  for decay onto the steady state. Also we have confirmed with a few runs on the Rheometrics machine (Bordeaux) that the relaxation times do not depend appreciably on which machine was used. This is true whenever  $\dot{\gamma} > \dot{\gamma}_1$  (the shear-banding region) where the slow transients are seen. For  $\dot{\gamma} < \dot{\gamma}_1$  (no shear bands), the relaxation is on the Maxwell time-scale, which can be resolved in the Rheometrics but not the Carrimed setup. (The curves are then different, but we are not interested in that regime in this paper.) The relaxation times  $\tau_{ss}$  do seem to depend appreciably on the cell geometry, being somewhat shorter in a Couette-Mooney cell than in a

Table II. —  $\tau_{ss}$  for the 100/75 system at various shear rates and temperatures. The data is for the Carrimed rheometer with a cone/plate cell. (Maxwell times given in Tab. I.)

$T$	$\dot{\gamma}\tau_M$	$\tau_{ss}/\tau_M$	$n$	$T$	$\dot{\gamma}\tau_M$	$\tau_{ss}/\tau_M$	$n$
19 °C	0.94	410	3	23.5 °C	0.94	435	2
	1.02	275	3		0.96	475	2
	1.10	230	3		0.99	550	2
	1.19	170	3		1.02	535	3
	1.27	145	3		1.05	425	3
	1.36	110	3		1.11	320	3
	1.45	90	3		1.14	285	3
	1.53	67	3				

Table III. —  $\tau_{ss}$  for the 100/60 system at 23.5 °C. The rheometer and cell geometry is as stated. (Maxwell time = 2.5 s).

cell	$\dot{\gamma}\tau_M$	$\tau_{ss}/\tau_M$	$n$	cell	$\dot{\gamma}\tau_M$	$\tau_{ss}/\tau_M$	$n$	cell	$\dot{\gamma}\tau_M$	$\tau_{ss}/\tau_M$	$n$
TA	1.0	-	-	TA	1.0	-	-	Rheo			
C/P	1.25	328	2.5	Couette	1.25	180	2.5	Couette	1.25	184	2
	1.5	136	2.5		1.5	92	2.5		1.5	72	2
	1.75	78	3		1.75	50	3		1.75	32	2
	2.0	58	3		2.0	34	3				
	2.25	44	3								

cone and plate cell. The reason for this is unclear, but may possibly be related to the greater inhomogeneity of the stress field in a Couette geometry, which could assist the formation of shear bands [17].

Some relaxation times  $\tau_{ss}$  for the 100/75 system are shown in Table II. Those measured at 19 °C are shown as a function of  $\dot{\gamma}$  in Figure 9. The curve is consistent with a power law divergence of the form

$$\tau_{ss} \sim |\dot{\gamma} - \dot{\gamma}_c|^{-p} \quad (2)$$

where  $p = 2.35-2.5$  and  $\dot{\gamma}_c = 0.355/\tau_M$  is a "critical" shear rate. (These parameters are best fit values.) Note however, that this critical shear rate is far less than  $\dot{\gamma}_1 = 0.85/\tau_M$ , as determined from the onset of the plateau region in Figure 6. This means that the relaxation time  $\tau_{ss}$  remains finite throughout the shear-banding region ( $\dot{\gamma} > \dot{\gamma}_1$ ). However, it is interesting, and suggestive, that it can be fit to a power law divergence, albeit with a "hidden" critical point  $\dot{\gamma}_c < \dot{\gamma}_1$ . It is possible that the data of Berret *et al.* [18] could also be fit this way, but they do not give enough values to try the comparison. On the other hand, our data for 100/75 at 23.5 °C does not support a similar fit (see Tab. II).

6.2. SYSTEM 100/60. — The behaviour in this case is extremely rich and interesting. Firstly, to fit some of the curves, values of  $n$  less than 2 or more than 3 are required. Also, at some shear-rates (especially at  $T = 20$  °C), the approach to the steady state appears to occur in more than one stage (with extra inflexions on the decay curves). However, for the purposes of

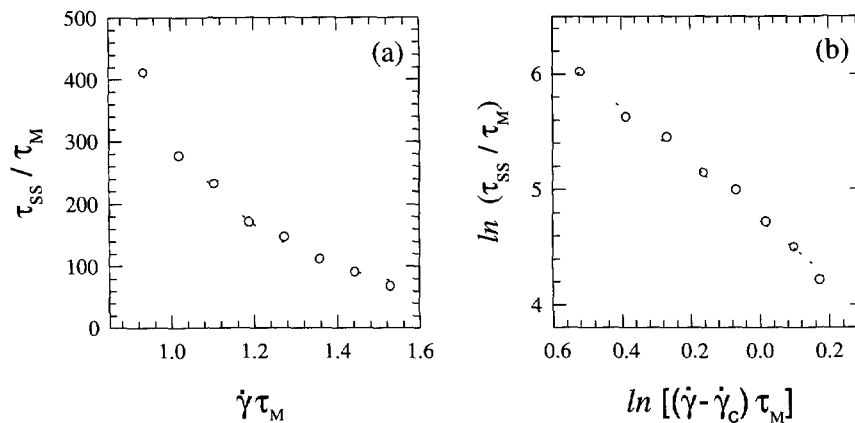


Fig. 9. — System 100/75 at 19 °C: Plot of the relaxation time  $\tau_{ss}$  versus  $\dot{\gamma}$ . (a) Linear/linear; (b)  $\ln/\ln$  with  $\dot{\gamma}_c\tau_M = 0.355$ .

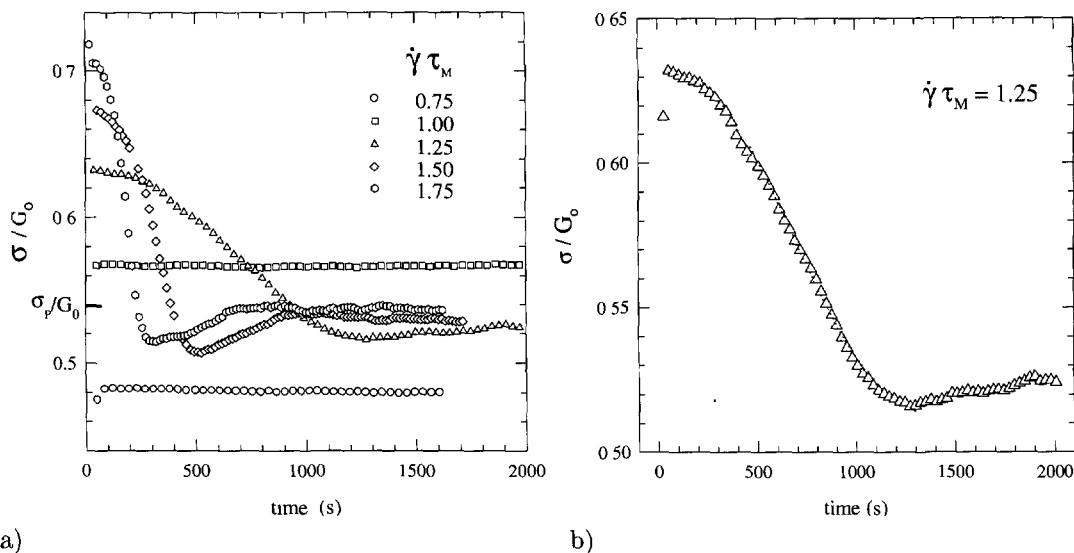


Fig. 10. — a) Transient response curves (startup of steady strain) for system 100/60 at 23.5 °C. Note the absence of decay for  $\dot{\gamma}\tau_M = 1.0$ ; this system shows a steady-state shear stress well above  $\sigma_p = 0.54G_0$ . (No decay is visible also for  $\dot{\gamma}\tau_M = 0.75$ ; however, this value lies below the onset of shear banding so the steady state is reached rapidly and has a stress less than  $\sigma_p$ .) b) Typical fit of relaxation curve ( $\dot{\gamma}\tau_M = 1.25$ ,  $n = 2.5$ ).

extracting  $\tau_{ss}$  it is usually possible to get a reasonable estimate fitting to a single-stage decay curve, with  $n$  around 2 or 3. Some values of  $\tau_{ss}$  for this system are shown in Table III. We also obtained data at  $T = 20$  °C, however the fits were less satisfactory due to the more complicated (multimodal) shapes of the relaxation curves. Accordingly we focus on the higher temperature dataset in what follows.

We show in Figure 10 the startup curves in a cone/plate cell for  $T = 23.5$  °C; curves were taken in order of increasing  $\dot{\gamma}$  with 5 minutes rest in between runs. (This was the

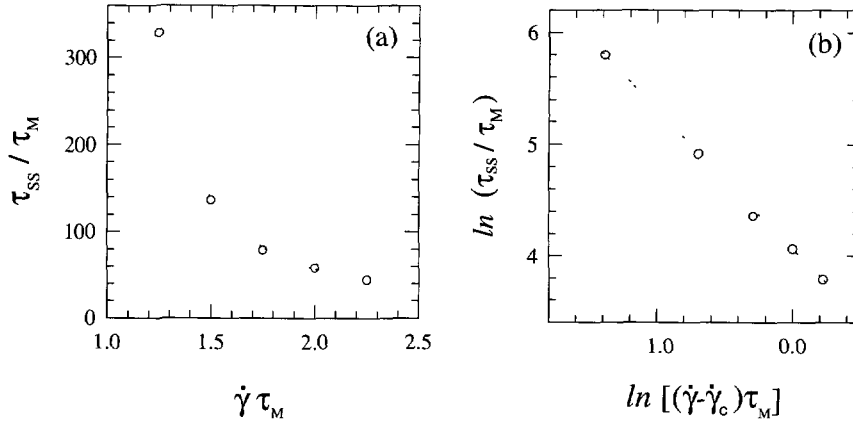


Fig. 11. — System 100/60 at 23.5 °C. Plot of the relaxation time  $\tau_{ss}$  versus  $\dot{\gamma}$ . (a) Linear/linear; (b)  $\ln/\ln$  with  $\dot{\gamma}_c \tau_M = 1.0$ .

usual procedure chosen; there was in some cases a slight difference between an increasing and decreasing sequence for the measurements. We also did some runs with 15 minutes rest in between; this led to some differences in relaxation times but no qualitative changes in the behaviour reported below.) We observe that curves with  $\dot{\gamma}$  well above  $\dot{\gamma}_1 = 0.85/\tau_M$  show a stress decay onto the plateau value  $\sigma_p = \sigma(\dot{\gamma}_1) = 0.54G_0$ . The decay times are quite slow (hundreds of seconds) and get slower for smaller  $\dot{\gamma}$ . However, there is one curve ( $\dot{\gamma}\tau_M = 1.0$ ) for which there is no apparent decay on the time-scale of hours. This curve seems to be “stuck” with a constant shear stress whose value is not  $\sigma_p$ . (This behaviour was already mentioned in discussing Fig. 7.) Moreover, this stress is reached already at rather early times (limited by initial transients unresolved by our setup), and corresponds to the stress arising during the “latency” period of the other curves. Hence, although the curve at first sight shows rapid relaxation onto a steady state, it is the “wrong” steady state; by comparison with the other curves, we see that this curve actually represents an *unmeasurably large*  $\tau_{ss}$ . Similar results were obtained on more than one occasion for shear rates close to this value.

To analyse the  $\dot{\gamma}$  dependence of  $\tau_{ss}$ , we have fit the measured values for the TA cone/plate setup (when finite) to the form of equation (2). The result is shown in Figure 11; our best estimates of the fit parameters are  $p = 1.2$  and  $\dot{\gamma}_c = 1.0/\tau_M$ . To within error from the fit, this  $\dot{\gamma}_c$  coincides with the value of  $\dot{\gamma}$  for the “stuck” flow curve measured in Figure 10. (Note that this correspondence was not forced:  $\tau_{ss}$  for this flow rate, being unmeasurably large, was *excluded* from the fit.) Although the power law exponent is different, this data is qualitatively like the 100/75 system *except* that  $\dot{\gamma}_c$  now exceeds  $\dot{\gamma}_1 = 0.85/\tau_M$ . Indeed from Figure 10 we have  $\sigma(\dot{\gamma}_c) = 0.57G_0$  whereas  $\sigma(\dot{\gamma}_1) = 0.54G_0$ ; although the difference is small it is unambiguous in the Figure (bear in mind that all these curves were taken with a single filling of the rheometer cell.) These data show that the divergence in  $\tau_{ss}$  is no longer “hidden”: it appears that instead a small window of strain rates has opened up ( $\dot{\gamma}_1 < \dot{\gamma} \leq \dot{\gamma}_c$ ) for which  $\tau_{ss}$  is unbounded. This situation is sketched in Figure 12.

We now discuss the relationship between  $\sigma_c$  and  $\sigma_{jump}$ . The critical stress  $\sigma_c$  was defined above in terms of the divergence of  $\tau_{ss}$  in a startup experiment at fixed strain rate. On the other hand,  $\sigma_{jump}$  for the 100/60 system was defined as the stress below which a startup experiment at controlled *stress* remains indefinitely in a metastable state. (Broadly speaking, this also corresponds to the onset of instability in a slowly increasing stress sweep measurement, as

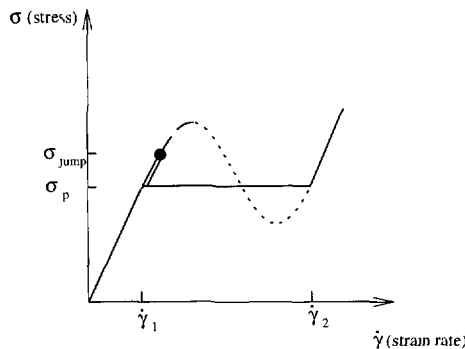


Fig. 12. — Apparent form of metastability/flow curve for 100/60 system. The unstable part of the stress *vs.* strain rate curve is dotted. The observed flow curve found *e.g.* on decreasing strain-rate sweep (solid). Metastable branch (double line): in this region the lifetimes  $\tau_{ss}$  of metastable states appear to be infinite. Metastable states can be observed beyond this point (dashed) but with a finite  $\tau_{ss}$  which diverges as the point marked • is approached.

discussed earlier.) In principle, the stress startup experiments could also be analysed to look for a divergence in the relaxation time, but this is *not* feasible in practice because a series of stresses could not be compared for a single filling of the rheometer (the sample would be ejected each time). In any case, without clear evidence to the contrary, it is simplest to assume that  $\sigma_{\text{jump}} = \sigma_c$ , as sketched in Figure 12. This means that the criterion for remaining indefinitely on the metastable branch, in a startup measurement, is independent of whether controlled stress or controlled strain rate is used. (Although the transient response on time-scale  $\tau_M$  is different in these two cases, the long time behaviour should be almost the same.) We believe our data to be consistent with this, although we cannot rule out the possibility that  $\sigma_{\text{jump}}$  and  $\sigma_c$  differ by a small finite amount. What is clear is that both are distinctly larger than the plateau stress,  $\sigma_p$ , causing a “window of metastability” to appear above  $\sigma_p$  (or  $\dot{\gamma}_1$ ) for which a metastable, unbanded flow can be maintained indefinitely.

Obviously, it is possible that  $\tau_{ss}$  is not actually infinite in this (stress or strain-rate) window: all we can say is that, if finite, the values of  $\tau_{ss}$  lie beyond our patience to measure them (we waited about  $10^4$  s). Even if finite, the behaviour of  $\tau_{ss}$  at least suggests a change of mechanism at  $\dot{\gamma}_c$ : whatever is the kinetic process by which bands are formed at high mean strain rates, this relaxation switches off as a power law at  $\dot{\gamma}_c$  and some other (unmeasurably slow) mechanism takes over. On the other hand, if the relaxation times for  $\dot{\gamma}_1 < \dot{\gamma} < \dot{\gamma}_c$  really are infinite, then it means that the final steady state achieved under an imposed mean flow rate  $\dot{\gamma}$  depends, not only on the value of  $\dot{\gamma}$ , but also on the way in which this mean flow was switched on in the distant past.

## 7. Discussion and Conclusion

Berret *et al.*'s proposal [18] of the Gaussian form for the relaxation function of stress under steady shear flow was based on an explicit model of nucleation and one-dimensional growth of nematic domains. This mechanistic interpretation appears less plausible for our systems which have very low weight fractions and are not close to any nematic phases on the static phase diagram. So it is all the more remarkable that we observe such similar relaxation curves (although we are forced to adopt a wider range of exponent  $n$  in the fits). Certainly, the

existence of a flat latency period, rather than a finite initial slope on the decay curves, are suggestive of a nucleation mechanism. Indeed, our data on the 100/75 system is overall quite similar to that of Berret *et al.* [18] and on this basis one might suggest that a nucleation mechanism was at work here too. Given that, for the 100/60 system, the relaxation time  $\tau_{ss}$  diverges at  $\dot{\gamma}_c$ , then that suggests something closer to a spinodal than a nucleation process. In spinodal decomposition, the relaxation time diverges at the spinodal point itself. For shallower quenches than this, the process is controlled by a slower (nucleation and growth) mechanism, whose relaxation time is normally finite but might conceivably be infinite here (this might depend on how the barrier to nucleation scales with system size).

However, this entire discussion relies on a dubious analogy with the thermodynamics of static phase transitions (see *e.g.* Ref. [19]). It seems likely that a proper explanation of the shapes of the startup curves and their corresponding  $\tau_{ss}$  values will have to await a detailed theory of exactly how shear-banded flows develop from an initially homogeneous flow. Neither the spinodal nor the nucleation terminology need be appropriate to the true process, which may involve the slow drift of a sharp band interface from one position to another in the cell [14, 16]. We have not examined in detail the dependence of the relaxation times  $\tau_{ss}$  on the cell geometry, but this mechanism would imply some such a dependence, which we do observe.

As mentioned previously, the CPyCl/NaSal system may be sensitive to impurity effects; this makes us cautious of any direct comparison with the earlier work of Rehage and Hoffmann on the 100/60 system [12]. Nonetheless, for the samples studied here, we have shown conclusively that the top-jumping scenario, whereby coexisting bands have the maximum possible shear stress, does not in fact provide the true selection criterion for these bands. This negates the simple assumption of top-jumping made by Spenley *et al.* [4] in their fit to the original Rehage/Hoffmann data. However, our data is in accord with more recent work on the mechanism of band selection based on interfacial stresses [14, 16], and with results of Berret *et al.* on a different system [18]. The absence of top-jumping was proved (for both the 100/60 and 100/75 compositions) by direct observation of a metastable branch of the underlying flow curve, in which the system reproducibly became trapped at a stress above the plateau value  $\sigma_p$ , for time scales much longer than the Maxwell relaxation time of the fluid. Moreover, in the 100/60 case we found evidence for a small window of shear rates or stresses in which the system remains on the metastable branch indefinitely ( $\geq 10^4$  s). As this window is approached from above, the relaxation time  $\tau_{ss}$  diverges with a power law; within the window, the ultimate state of stress apparently depends on the flow history of the sample in the indefinitely remote past. Recent theories on the dynamics of band selection clearly lead one to expect departures from top-jumping [14, 16–19], and in some cases anticipate that metastable unbanded flows are possible. However, the factors controlling the lifetime of these metastable states are not yet known, so it remains to be seen whether any of these theories can explain the richness of the behaviour we have observed.

## Acknowledgments

We thank J.-F. Berret, P. Callaghan, S.J. Candau, C.-Y. D. Lu, T. McLeish, P. Olmsted, H. Rehage and J.B.A. Smeulders for useful discussions prior to or during this work. We especially thank Wilson Poon and Didier Roux for their help and encouragement. This work was funded in part under EC TMR Network CT94-0696 and in part under EPSRC Grant GR/K 59606.

## References

- [1] Cates M.E. and Candau S.J., *J. Phys. Condens. Matt.* **2** (1990) 6869; see also Cates M.E., in *Structure and Flow in Surfactant Solutions*, C.A. Herb and R.K. Prud'homme, Eds., Symposium Series 578 (ACS Books, Washington, 1994).
- [2] Cates M.E., *Macromolecules* **20** (1987) 2289.
- [3] Cates M.E., *J. Phys. Chem.* **94** (1990) 371.
- [4] Spenley N.A., Cates M.E. and McLeish T.C.B., *Phys. Rev. Lett.* **71** (1993) 939; see also McLeish T.C.B. and Ball R.C., *J. Polym. Sci. Polym. Phys. Edn.* **24** (1986) 1735; McLeish T.C.B., *J. Polym. Sci. Polym. Phys. Edn.* **25** (1987) 2253.
- [5] Yerushalmi J., Katz S. and Shinnar R., *Chem. Eng. Sci.* **25** (1970) 1891.
- [6] Cates M.E., McLeish T.C.B. and Marrucci G., *Europhys. Lett.* **21** (1993) 451; Spenley N.A. and Cates M.E., *Macromolecules* **27** (1994) 3850; Marrucci G., *J. Non-Newton. Fluid Mech.* **62** (1996) 279; Ianniruberto G. and Marrucci G., to be published.
- [7] Makhloufi R., Decruppe J.P., Ait-Ali A. and Cressely R., *Europhys. Lett.* **32** (1995) 253; Decruppe J.P., Cressely R., Makhloufi R. and Cappelaere E., *Colloid Polym. Sci.* **273** (1995) 346.
- [8] Mair R.W. and Callaghan P.T., *Europhys. Lett.* **65** (1996) 241.
- [9] Callaghan P.T., Cates M.E., Rofe C.J. and Smeulders J.B.A.F., *J. Phys. II France* **6** (1996) 375.
- [10] Mair R.W. and Callaghan P.T., to be published.
- [11] Britton M.M. and Callaghan P.T., to be published.
- [12] Rehage H. and Hoffmann H., *Molecular Phys.* **74** (1991) 933; Rehage H. and Hoffmann H., *J. Phys. Chem.* **92** (1988) 4712.
- [13] See e.g. Khatory A., Lequeux F., Kern F. and Candau S.J., *Langmuir* **9** (1993) 1456.
- [14] Spenley N.A., Yuan X.-F. and Cates M.E., *J. Phys. II France* **6** (1996) 375; see also Espanol P., Yuan X.-F. and Ball R.C., *J. Non-Newton. Fluid Mech.* **65** (1996) 93.
- [15] El-Kareh A.W. and Leal G.L., *J. Non-Newton. Fluid Mech.* **33** (1989) 257; Brunovsky P. and Sevcovic D., *Q. Appl. Math.* **L2** (1994) 401.
- [16] Olmsted P.D. and Lu C.-Y.D., to be published.
- [17] Greco F. and Ball R.C., *J. Non-Newton. Fluid Mech.*, in press; see also Schmitt V., Lequeux F. and Marques C.M., *Langmuir* **10** (1995) 4009.
- [18] Berret J.F., Roux D.C., Porte G. and Lindner P., *Europhys. Lett.* **25** (1994) 521; Berret J.F., Roux D.C. and Porte G., *J. Phys. II France* **4** (1994) 1261.
- [19] Porte G., Berret J.-F. and Harden J.L., *J. Phys. II France* **7** (1997) 459.
- [20] Rehage H. and Candau S.J., private communications.
- [21] Turner M.S. and Cates M.E., *Langmuir* **7** (1991) 1590.